Journal of Nanoscience and Technology 2(1) (2016) 43–49

ISSN: 2455-0191

Contents List available at JACS Directory

Journal of Nanoscience and Technology

journal homepage: www.jacsdirectory.com/jnst

Composite Ion-Exchangers Based On Flexible Resin Containing Zirconium Hydrophosphate for Electromembrane Separation

Y.S. Dzyazko[1,*], Y.M. Volfkovich[2], L.N. Ponomaryova[1], V.E. Sosenkin[2], V.V. Trachevskii[3], V.N. Belyakov[1]

[1]*V.I. Vernadskii Institute of General and Inorganic Chemistry of the NAS of Ukraine, Acad. Palladin ave. 32/34, Kyïv-142, 03680, Ukraine.*
[2]*A.N. Frumkin Institute of Physical Chemistry and Electrochemistry of the RAS, Leninskii pr, 31, Moscow, 119071, Russia.*
[3]*G.V. Kurdyumov Institute for Metal Physics of the NAS of Ukraine, Pr. acad. Vernaskii 36, Kyïv-142, 03680, Ukraine.*

GRAPHICAL ABSTRACT

Ion Transport Through Organic-Inorganic Ion-Exchangers Affected by Single Nanoparticles of Zirconium Hydrophosphate

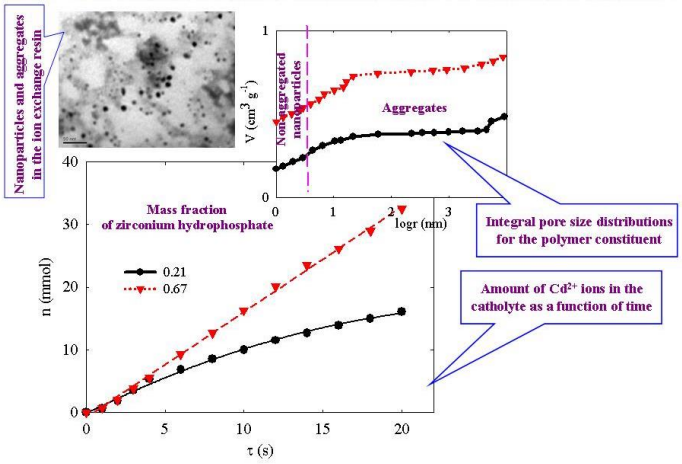

ARTICLE DETAILS

Article history:
Received 25 October 2015
Accepted 02 November 2015
Available online 12 November 2015

Keywords:
Electrodeionization
Electrodialysis
Organic-Inorganic Ion-Exchanger
Zirconium Phosphate
Standard Contact Porosimetry

ABSTRACT

Organic-inorganic materials based on flexible gel-like cation exchange resin were obtained by means of its modification with zirconium hydrophosphate. The samples were investigated using transmission and scanning electron microscopy, standard contact porosimetry as well as impedance spectroscopy. Single nanoparticles (4-10 nm) and their aggregates were found inside the polymer. Evolution of porous structure of the polymer constituent affected by the inorganic particles is considered, the modifier has been shown to decrease the content of free water in the polymer, to increase swelling pressure, which is determined according to Gregor model, and to provide a growth of ion-exchange capacity in a comparison with the pristine resin (from 0.56 up to 2.3 mmol cm^{-3}). The inorganic constituent formally behaves like a cross-linking agent. However, increasing of the modifier amount causes a growth of electrical conductivity of the composites from 0.2 to 0.8 $Ohm^{-1}m^{-1}$. The ion-exchanger with a maximal content of zirconium phosphate (67 %) was applied to removal of Cd^{2+} ions from a solution containing also hardness ions and organics. The composite provide continuity of the process, the removal degree of toxic ions reaches 96-98%. Redistribution of the nanoparticles in the polymer, which is affected by electric field, has been found.

1. Introduction

In opposite to electrodialysis, electrodeionization (EDI) involves not only membranes, but also granulated ion-exchange resins between them: cation-exchanger, anion-exchanger or their mixture [1-3], particularly layered bed [4]. Simultaneous ion exchange and transport of sorbed species through the ion-exchanger bed and membranes provide continuity of the EDI process. This hybrid technique is applied to weakly-concentrated solutions, since the ion-exchanger particles intensify mass transport. The EDI method allows one to solve different tasks, such as treatment of reverse osmosis permeate [4], production of ultrapure water [5], removal of Ni^{2+} [6-12], $HCrO_4^-$ [13-16], Cu^{2+} [17-19] ions from electroplating wastes, recovery of Co^{2+} [20] and Cs^+ [21] ions from water produced by of nuclear stations, F^- anions removal from tap water [22], water softening [23] etc.

Removal of heavy metal ions from diluted solutions is complicated by low selectivity of ion exchange resins and their poisoning with organics [6]. In order to overcome these difficulties, glass-like hydrogel of zirconium hydrophosphate (ZHP) has been proposed [8]. A disadvantage of this ion-exchanger is gradual fragmentation of grains.

Organic-inorganic ion-exchangers are widely used for removal of heavy metal ions from diluted solutions by means of ion exchange [10, 24-28].

*Corresponding Author
Email Address: dzyazko@gmail.com (Y.S. Dzyazko)

Cite this Article as: Y.S. Dzyazko, Y.M. Volfkovich, L.M. Ponomaryova, V.E. Sosenkin, V.V. Trachevskii, V.N. Belyakov, Composite ion-exchangers based on flexible resin containing zirconium hydrophosphate for electromembrane separation, J. Nanosci. Tech. 2(1) (2016) 43–49.

The material based on flexible resin was also applied to the EDI process of Ni^{2+} removal from a combining weakly-concentrated solution [10], the composite consisting of ammonium molybdophosphate and polyacrylonitrile has been proposed for EDI of Cs^{+}-containing solutions [21]. However, the process efficiency was rather low. In order to overcome this disadvantage, functional properties of the ion exchanger, namely electrical conductivity and ion exchange capacity, have to be improved.

These properties are known to be determined by location of nanoparticles in one or other pores of the polymer matrix [26, 28]. Porous structure of swollen ion-exchange polymer includes several types of pores [29-31]. Gel fields of the polymer are riddled with nanosized pores so called "transport pores" (clusters and narrower channels between them), where functional groups are placed. These pores are responsible for ion movement. Non-aggregated nanoparticles in clusters and channels enhance the transport. Hydrophobic links of the polymer chains are located in voids between gel fields, a size of which is more than 20 nm. The largest pores are the structure defects.

The aim of the investigation is a purposeful control of a state of the inorganic constituent in ion exchange polymer in order to provide maximal content of non-aggregated nanoparticles in transport pores. The purpose of the study is also to establish the influence of the particles on the polymer structure and functional properties of the composites. At last, testing of the materials in the EDI process is necessary.

Flexible gel-like cation exchange resin has been chosen as a polymer matrix, since this material can be used successfully for removal of d-metal ions by means of EDI [6]. Macroporous and rather rigid ion exchange polymers were used earlier for composite preparation, mainly aggregated nanoparticles were found for these materials [24, 25, 28]. In this study, ZHP was used as a modifier, since it provides selectivity of the composites [10, 24, 26, 28] due to formation of complexes of sorbed ions with functional groups of this ion-exchanger [32, 33].

The composites were tested for removal of Cd^{2+} ions from multicomponent solution containing also hardness ions and organics. The equipment, which contains details with cadmium coatings, is attractive for petroleum, automotive, electric and electronic industries especially for shipbuilding [34]. This is due to variable properties of cadmium coatings: stability against corrosion, low friction coefficient etc. In owing to high toxicity of cadmium ions, their removal from electroplating wastes is an important task.

2. Experimental Methods

2.1 Ion-Exchangers

Such strongly acidic cation-exchanger as Dowex WX-2 (*Dow Chemical*), which contains 2 % DVB, was used as a polymer matrix. Further the resin is marked as *CR*.

The modification procedure involved: (i) swelling a weighted amount of the resin in deionized water; (ii) impregnation with a 1 M $ZrOCl_2$ solution for 24 h at 353 K followed by separation of solid and liquid by means of centrifugation: (iii) treatment with a 1 M H_3PO_4 solution at 273 K and phase separation, washing with deionized water up to pH 7 of the effluent; (iv) drying under vacuum at 343 K followed by a treatment with ultrasound at 30 kHz using a *Bandelin* ultrasonic bath (*Bandelin*); (v) drying in a desiccator over $CaCl_2$ at 293 K down to constant mass. The differences of this technique from [10, 26] is higher temperature of impregnation with a zirconium-containing solution and lower temperature of ZHP precipitation.

The (i)-(v) procedures were repeated several times. After each modification cycle, a weighted sample was taken for investigations. The samples, which were researched in detail, were marked as *CR-ZHP-1* (one modification cycle) and *CR-ZHP-7* (seven cycles). The *CR-ZHP-0* sample modified one time under room temperature similarly to [10] was also studied for a comparison.

2.2 Visualization of Inorganic Particles

Pretreatment of the ion-exchangers involved their grinding followed by ultrasonic treatment. TEM images were obtained by means of a *JEOL JEM 1230* transmission electron microscope (*Jeol*).

A *JEOL JSM 6700 F* scanning electron microscope (*Jeol*) was also used for ZHP visualization. Preliminarly an ultrathin layer of platinum was deposited onto the particles at 3 Pa using an *JEOL JFC-1600* Auto fine coater (*Jeol*).

2.3 Porosity Measurements

Standard contact porosimetry (SCP) [35-38], which has been recognized by the IUPAC [35], was applied to investigation. Preliminary the samples were vacuumed at 353 K, weighted and put into a paper tablet. The tablet was placed between two ceramic standards, the set was impregnated with deionized water at 353 K. The contact between the investigated and standard samples was provided at 0.1 kPa. During drying at 293 K, the set was disassembled periodically, each its element was weighted. Based on the experimental results of mass loss, the pore size distributions as well as isotherms of water adsorption were plotted taking into consideration a known contribution of the paper.

Archimedes (picnometer) method [39] was also used to determine total porosity and particle density.

2.4 Chemical Composition

The content of phosphorus and zirconium inside the samples was determined with powder analysis using an X-Supreme8000 XRF (X-ray fluorescence) spectrometer (Oxford Instruments). NMR ^{31}P spectra of the samples, which had been inserted into the ampule with a diameter of 5 mm, were obtained by means of *AVANCE 400* spectrometer (*Bruker*) using single-pulse technique under the accumulation mode at 162 MHz. Chemical shift has been determined relatively to 85 % H_3PO_4.

2.5 Functional Properties

Total ion-exchange capacity of the materials towards Na^{+} (*A*) was determined by their treatment with a 0.1 M NaOH solution followed by washing with deionized water, regeneration and flame-photometric analysis of the effluent [10].

Electrical conductivity of H-forms of the ion-exchangers was measured at 298 K similarly to [40]. Preliminary additionally sorbed electrolyte was removed from the solid by multiple washing with deionized water. The sample was placed into a prismatic cell supplied by platinum electrodes (an area of each electrode was 2 cm^2, a distance between them was 1 cm). The cell with the ion-exchanger was filled with deionized water. The admittance spectra within the interval of 10^{-2}-10^{6} Hz were obtained using an *Autolab* impedance system. The *dc* conductivity of the bed was determined from the wide plateau of real part of admittance similarly to [41].

2.6 Electrodeionization

The experimental set-up [7, 13] involved a three-compartment electrodialysis cell, 3 independent liquid lines, power supplier and measurement instrumentation. Geometric parameters of the space between the membranes (central compartment), where the ion-exchanger was placed, were as follows: an effective membrane area was 16 cm^2, a distance between the membranes was 1 cm, a height of the ion-exchanger bed was 16 cm. A top of the cell was opened to provide a possibility of bed compaction in order to avoid its fluidization.

The electrode compartments were separated from the centre chamber with homogeneous Nafion 117 cation-exchange membranes (DuPont). A 1 M H_2SO_4 solution circulated though the anode compartment, the cathode camera was filled with a 1 M HCl solution. A volume of both catholyte and anolyte was 200 cm^3.

Tap water containing 1.2 mmol dm^{-3} Ca^{2+}, 0.5 mmol dm^{-3} Mg^{2+} and also organics (mainly humates) was used for preparation of a Cd^{2+}-containing solution (0.5 mmol m^{-3} Cd^{2+}) after preliminary acidification down to pH 2.5. The solution passed through the central compartment according to "once through" scheme with a flow velocity of 60 cm^3 min^{-1}. The process was performed at 8 V, probes (2 cm^3) from the cathode and central compartments were analyzed with an atomic absorption method using a *Pye Unicam SP9* spectrophotometer.

The EDI processes have been performed for 20 h, in the case of the *CR-ZHP-7* sample the process was repeated 5 times. After each experiment, the ion-exchanger was removed from the cell, washed with a 1 M H_2SO_4 solution and deionized water, further this ion exchanger was used again. Particle density of the samples was determined with Archimedes method after each series of EDI-regeneration. After the fifth experiment, the sample (marked as *CR-ZHP-7-ED*) was investigated using a SCP technique.

The *CR-ZHP-7* ion-exchanger (1 g) was also treated with a Cd^{2+}-containing solution of abovementioned composition (1 dm^3), regenerated, further its particle density was determined. This procedure (blank experiment) was repeated 5 times.

3. Results and Discussion

3.1 ZHP Precipitation inside Ion Exchange Polymer

Zirconium ions forms polymerized hydroxocomplexes in aqueous media, such as $[Zr_4(OH)_8(H_2O)_{16}]_x^{8+}$ (where *x* is the integer), their composition strongly depends on the solution pH [42]. During impregnation of the resin with a highly concentrated $ZrOCl_2$ solution, a part of species is sorbed according to ion exchange mechanism. The ion-

exchanger contains also both cations (zirconium hydroxocomplexes as well as H^+) and anions (Cl^-), which are sorbed additionally.

Polymer chains of the pristine resin are visible in Fig. 1a. Regarding the organic-inorganic ion-exchanger modified at low temperature, the chains are invisible, however, particles of the modifier can be observed: non-aggregated spherical nanoparticles (4-10 nm) and their aggregates of irregular shape (Fig. 1b). Single nanoparticles are evidently located in transport pores and stabilized by their walls [26]. Large aggregates of micron size are formed inside structure defects (Fig. 1c,d). The sample, which was treated with phosphoric acid at higher temperature, shows mainly aggregated nanoparticles (Fig. 1e).

The smallest ZHP particles are dissolved during precipitation in accordance with Ostwald-Freundlich equation [43]:

$$\ln\frac{C}{C_\infty}=\frac{\beta v_m\sigma\cos\varphi}{RTr}. \quad (1)$$

Here C is the compound concentration, C_∞ is the concentration of saturated solution, β is the shape factor of particles, v_m is the molar volume of the compounds, σ is the surface tension of the solvent, φ is the wetting angle, R is the gas constant, T is the temperature, r is the particle radius. In the case of hydrophilic compounds like ZHP, cos φ is assumed to be equal 1.

Since the C and C_∞ values for insoluble ZHP are extremely low, a size of the dissolved particles is affected mainly by temperature conditions. Decreasing in the temperature prevents dissolution of the smallest particles. In the case of higher temperature, dissolution of small particles and reprecipitation of larger formation occur. In other words, the control of temperature allows us to obtain ZHP particles in one or the other pores of the polymer matrix.

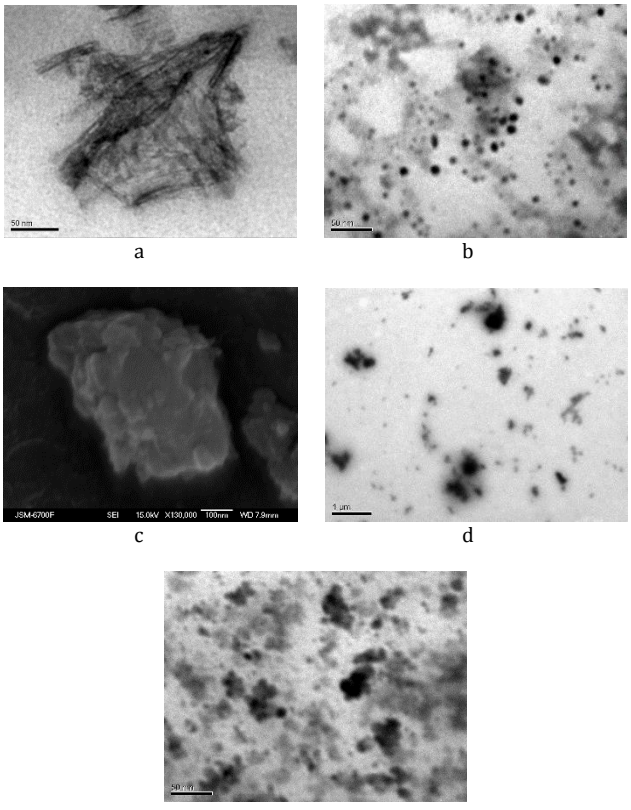

Fig. 1 Microphotographs of the *CR* (a), *CR-ZHP-1* (b, c), *CR-ZHP-7* (d) and *CR-ZHP-0* (d) samples. TEM images (a, b, d, e) show non-aggregated nanoparticles of ZHP and their small aggregates. Large aggregates are seen in SEM (c) and TEM (d) images.

Impregnation of the resin with a $ZrOCl_2$ solution at elevated temperature leads to an increase of the modifier content in the polymer and results in a growth of ion exchange capacity per volume unit (A_v) of the composites (Fig. 2). This is evidently due to higher content of zirconium-containing species sorbed according to non-exchange mechanism. Inconsiderable growth of the ZHP content after the fifth modification cycle is probably due to formation of secondary porosity inside the polymer matrix. Small pores between the nanoparticles in the aggregates can be a barrier against additionally sorbed electrolyte, when the resin is treated with $ZrOCl_2$ or H_3PO_4 solutions. Increasing in mass fraction (m) of incorporated ZHP causes an increment of ion exchange capacity. The A_v-m plots show 2 regions: slow growth (due to considerable swelling of the composite [26, 28]) and rapid increase (due to decrease of swelling).

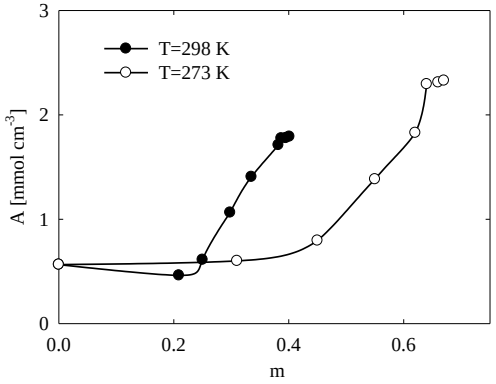

Fig. 2 Ion exchange capacity of the composites per volume unit as a function of mass fraction of ZHP. Legend shows temperature of the modifier precipitation. The curve for the samples obtained under room temperature was plotted according to data [10].

The samples, in which the modifier was precipitated at 273 K, are characterized by lower content of phosphorus in a comparison with the *CR-ZHP-0* composite (Table 1). Moreover, increasing of ZHP content causes a decrease of molar ratio of P:Zr due to effect of secondary porosity against H_3PO_4 as mentioned above. Larger exchange capacity of the *CR-ZHP-1- CR-ZHP-7* samples in a comparison with the resins obtained under room temperature is caused by larger content of the modifier.

Table 1 Characteristics of ion-exchangers

Sample	Molar ratio of P:Zr	Particle density, kg m^{-3}	A_m, mmol g^{-1}	Pore volume, cm^{3}cm^{-3}	A_{H_2O}', mmol g^{-1}*	n	P/P_s**
CR	–	1750	4.51	0.92	2.41	30	<0.20
CR-ZHP-0	1.60:1	1960	1.44	0.69	0.39	6***	0.99
CR- ZHP-1	1.52:1	2060	1.93	0.79	0.75	13	0.94
CR- ZHP-7	1.35:1	2530	4.29	0.78	0.78	29	0.94
CR- ZHP-7-ED	1.26:1	2120	2.30	0.77	1.11	24	0.21

**Before sharp build-up of the isotherm*

*** A_{H_2O} = 0.7 cm^{3}g^{-1}.*

****m = 0.28 [10].*

NMR ^{31}P spectroscopy was used for analysis of composition of the inorganic ion-exchanger. Typical spectrum for ZHP, which is incorporated into the polymer, is given in Fig. 3. The spectrum demonstrates intensive signal at -36 ppm, a shoulder in the region of weak field is also visible. As known for crystalline modifications of ZHP, the signal in a strong field is attributed to $(-O)_2PO_2H$ groups (α-modification), the signal in a weak field is due to $-OPO_3H_2$ groups (γ-modification) [44]. In our case, hydrophosphate groups dominate, the signal caused by dihydrophosphate groups appears as a shoulder.

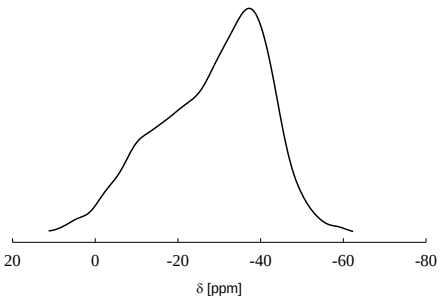

Fig. 3 NMR ^{31}P spectra of the CR- ZHP-7 sample

3.2 Porosity of the Polymer Constituent and Isotherms of Water Adsorption

Since the conditions of thermal pre-treatment before the porosity measurements cannot provide removal of bonded water from ZHP surface, the results are related mainly to the polymer constituent. Particle density of the ion-exchangers (ρ_p) was calculated as [39]:

$$\varepsilon=1-\frac{\rho_b}{\rho_p}, \quad (2)$$

where ε is the porosity, ρ_b is the bulk density. Insertion of ZHP predictably causes an increase of particle density (Table 1).

The exchange capacity per mass unit (A_m) of the composites is lower comparing with *CR*. It is evidently due to blockage of transport pores with the particles. As a result, functional groups are partially unavailable for ion exchange.

In opposite to well-known method of water adsorption isotherm [45], which is widely used for investigation of ion-exchange polymers, the SCP technique allows us investigate porous structure in a wide diapason of pore size. Nitrogen adsorption and mercury porosimetry are not able to give exact information about swollen polymers, since these methods can be applied only to dry materials.

Isotherms of water adsorption (A_{H_2O}) for the pristine ion-exchanger are typical for the materials containing a wide spectrum of pores. A long plateau at low P/P_s values is attributed to micropores (here P is the pressure of water vapour, P_s is the pressure of saturated vapour), semi-waves (mesopores) and extended vertical region at $P/P_s \rightarrow 1$ related to meso- and macropores (Fig. 4). At the same time, the isotherms for the modified ion-exchangers show mainly micropores. Meso- and macropores are less expressed in a comparison with the pristine resin.

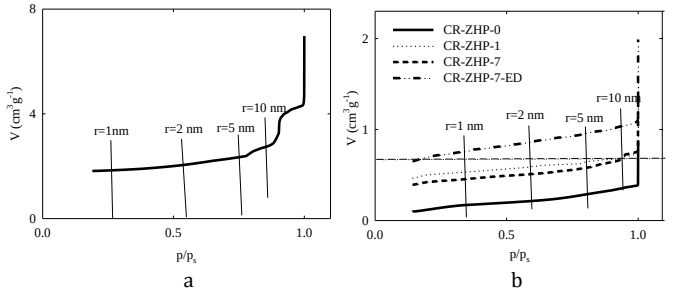

Fig. 4 Isotherms of water adsorption for the pristine resin (a) and composites (b). Insertion of ZHP into the polymer deteriorates water adsorption.

Horizontal branches of the isotherms are attributed to adsorbate monolayer. An amount of water molecules (n) in hydrate shells of counter-ions (H^+) of $–SO_3H$ groups was calculated as:

$$n = \frac{A_{H_2O}}{A_p V_{H_2O}} \quad (3)$$

for the pristine ion-exchanger and:

$$n = \frac{A_{H_2O}}{A_p V_{H_2O}(1-m)} \quad (4)$$

for the composites. Here V_{H_2O} is the molar volume of water, A_p is the exchange capacity of the pristine polymer. The highest n value has been found for the pristine ion-exchanger (Table 1). In general, modification results in a reduction of this parameter. However, increase of ZHP content causes an increment of the n value (compare *CR-ZHP-0* and *CR-ZHP-7*).

Let us consider thermodynamic aspects of swelling. Transport pores of the ion-exchangers contain high amount of counter-ions (H^+), which tend to solvation. It is possible to assume, that there is a solution of concentrated electrolyte inside transport pores, the "solution" is able to be diluted. This assumption is the closest to reality, when the ion-exchanger is in a contact with a weakly concentrated solution or deionized water. In this case, diffusion parts of intraporous double electric layers are overlapped in clusters. Thus, transport pores are filled with a "solution" completely. In macroscopic models, the tendency of the "solution" to be diluted is taken into consideration by a difference between osmotic pressures of liquids inside and outside granules (Gregor model [45]). It has been postulated, that the osmotic pressure inside ion-exchanger is higher, when the sample is equilibrated with a solvent or its vapour. A difference between the pressures is the swelling pressure, π. This value has been suggested for the ion-exchangers, which change their volume freely. According to the Gregor model, the π magnitude has not to be related to the swelling pressure of gel in a volume bounded with rigid walls.

When water content in the ion-exchanger increases, osmotic pressure decreases. At the same time, pressure from a side of the polymer net grows. These pressures become equal under equilibrium conditions.

The interrelation between the P/P_s value and swelling pressure, which is defined from the Gregor model, is written as [45]:

$$\pi v_{H_2O} = RT \ln \frac{P/P_s}{a_{H_2O}}. \quad (5)$$

Here a_{H_2O} is the activity of water in ion-exchanger, which is associated with free water. For instance, at A_{H_2O} =0.7 mmol g^{-1}, the P/P_s value decreases in the order: *CR-ZHP-0* > *CR- ZHP-1* ≥ *CR- ZHP-7* > *CR.* This order can be caused by a decrease of swelling pressure or water activity.

3.3 Pore Size Distributions

Insertions of Fig. 5 illustrate integral pore size distributions, namely dependencies of pore volume (V) on logarithm of pore radius (r). Differential distributions are given in Fig. 5. An area of each peak corresponds to a volume of one or another type of pores.

Regarding the pristine ion-exchanger, several peaks are observed (Fig. 5a). The broad maximum at log r =0.3 (nm) evidently corresponds to channels, the narrower peak (log r =0.7 (nm)) is attributed to clusters, the most sharp maximum at log r =0.7 (nm) is caused by voids between gel fields. The maxima at log r =2.8 and 3.6 (nm) are due to structure defects. The peak at log r >4 (nm) is attributed to voids between the ion-exchanger grains, these pores will be outside our attention.

The pore size distributions for the *CR-ZHP-0* sample demonstrates a shift of peaks, which are attributed to channels and clusters, towards lower log r values (to log r =0.2 and 0.5 (nm) respectively). A size of pores, which are free from functional groups, increases (log r =1.1 (nm) for voids between gel fields, log r =3.1 and 3.7 (nm) for structure defects).

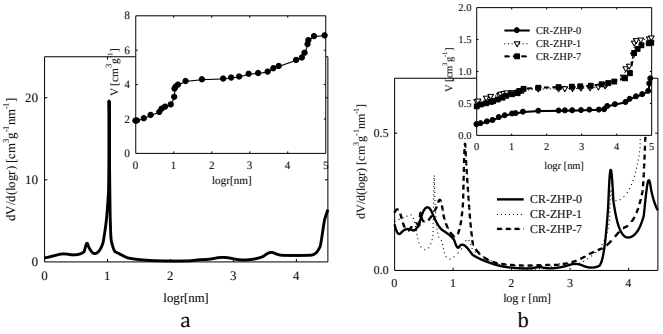

Fig. 5 Integral (insertions) and differential pore size distributions for the pristine resin (a) and composites (b). Modification results in transformation of porous structure of the polymer constituent.

Increase of fraction of non-aggregated nanoparticles (*CR-ZHP-1*) causes a shift of the peaks, which are related to transport pores and voids between gel fields, towards a region of higher log r values. These peaks become narrower. The composite shows broader peaks of structure defects, but a size of these pores remains without changes.

Regarding the *CR-ZHP-7* sample, a size of channels decreases, clusters become larger in a comparison with *CR-ZHP-1*. Moreover, these peaks are split. No change of a size of voids between gel fields has been found, though their volume increases. At last, the peaks, which correspond to structure defects, become too broad and practically unexpressed.

Pores, a radius of which is less than 1.5 nm (log r =0.17 (nm)), contain only bonded water, larger pores contain both bonded and free water [30]. A volume of larger pores (r>1.5 (nm)) reflects water activity in the ion-exchanger. Fig. 6 illustrates the volume of these pores for different ion-exchangers (for equilibrium state) as a function of P/P_s value at A_{H_2O} =0.7 mmol g^{-1}.

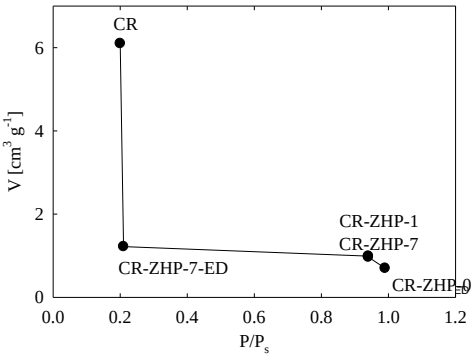

Fig. 6 Volume of pores, which contain free water (under equilibrium conditions) as a function of the P/P_s ratio, which corresponds to A_{H_2O} =0.7 mmol g^{-1}. Modification decreases the content of free water.

In a comparison with the pristine resin, the composites are characterized by lower volume of pores containing free water. Thus, larger P/P_s values for the organic inorganic ion-exchanger can be due to lower a_{H_2O} magnitude and higher swelling pressure (formula 5).

Among the *CR-ZHP-0*, *CR-ZHP-1* and *CR-ZHP-7* composites, no considerable change of the P/P_s ratio and volume of pores containing free water has been found. Thus, the swelling pressure for these samples is practically similar even under equilibrium conditions ($\pi v_{H_2 0} = -RT \ln a_{H_2O}$ [45]). However, a difference between the amounts of water molecules of counter-ions is sufficient (Table 1). Moreover, a change of pore size is also observed (Fig. 5).

This is evidently due to various swelling pressure in different pores, which is caused by a presence of ZHP. Indeed, a change of amount of osmotically active species (counter-ions of hydrophosphate groups) in one or the other pores affects swelling pressure inside them. If the main amount of ZHP is localized in structure defects, they are able to squeeze the transport pores and pores between gel fields (transition from *CR* to *CR-ZHP-0*). Lower *n* value can be due to partial inaccessibility of transport pores for water adsorption and ion exchange (decrease of ion exchange capacity per mass unit, Table 1). As a result, the A_p magnitude, which is used for calculations, is overestimated.

Preferable deposition of ZHP inside clusters and voids between gel fields (transition from *CR-ZHP-0* to *CR-ZHP-1* and *CR-ZHP-7*) evidently causes higher swelling pressure inside these pores than that in structure defects. Changes of swelling pressure inside different pores are evidently compensated (similarity of the P/P_s ratios and free water content). A part of transport pores become available for water adsorption and ion exchange (increase on the A_m and *n* values).

3.4 Electrical Conductivity

The impedance measurements were carried out for a packed bed. Thus, the resistance value, which is obtained by this manner, includes also the resistance of the grain boundaries. In owing to this, the conductivity is evidently less than those for "monoliths". However, the data reflect a relative change of conductivity affected by the inorganic modifier.

Fig. 7 illustrates the dependence of ion-exchanger conductivity (κ) on concentration of free mobile charge (H^+), i.e. on ion-exchange capacity. In general, modification leads to the conductivity growth. The samples, in which ZHP was precipitated at low temperature, are characterized by higher conductivity, than those modified under room temperature.

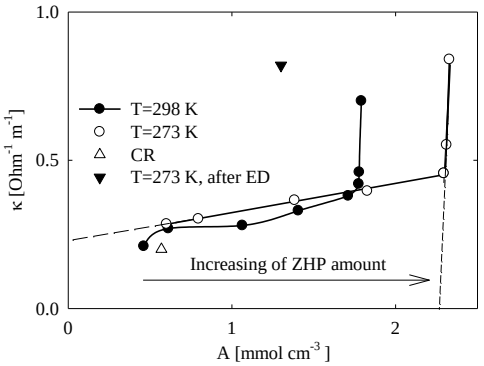

Fig. 7 Electrical conductivity of the ion-exchangers as a function of their ion exchange capacity. The curve for the samples obtained under room temperature was plotted according to data [10]. Legend shows temperature of the modifier precipitation.

In opposite to the composites based on the resin containing 8% DVB [26, 28], all materials demonstrate a build-up of conductivity with increasing of ZHP content (slow and rapid growth of the κ value). Extrapolation of the curve branches to the abscissa axis gives A <0 (slow growth) and A>>0 (rapid growth). A slow growth is evidently caused by transformation of porous structure of the polymer as well as by the modifier, which is characterized by slower ion transport than the flexible resin. Fast growth of the conductivity can be due to nanoparticles inside transport pores, since counter-ions of hydrophosphate groups are involved into ion transport. However, A>>0 at κ=0, this indicates no contribution of nanoparticle aggregates to the conductivity, since these formations are located outside transport pores of the polymer.

3.5 Electrodeionization

Fig. 8 illustrates the amount of Cd^{2+} ions in the cathode compartment (n_c) as a function of time (τ). As seen, the rate of ion transport through the ion-exchanger bed and membrane decreases in the range *CR-ZHP-7>CR> CR-ZHP-1> CR-ZHP-0.* Among the composites, the order coincides to conductivity (Fig. 7). The pristine resin shows higher rate of ion transport in a comparison with the composites containing low amount of the modifier. This is evidently due to inhibitory effect of ZHP, which squeeze transport pores of the polymer. Moreover, movement of species through clusters and channels can be complicated by additional interaction with functional groups of ZHP. The highest rate of ion transport, which is observed for *CR-ZHP-7*, is probably due to high amount of Cd^{2+} species sorbed by non-aggregated nanoparticles.

In the case of the *CR-ZHP-7* sample, the rate of ion transport was found to be constant. Thus, a flux of Cd^{2+} ions (N_c) calculated as $\frac{1}{A_e}\frac{dn_c}{d\tau}$ (where A_e is the effective area of the membranes) remains without changes within a wide range of time. No sufficient change of flux is observed from cycle to cycle of the EDI processes followed by chemical regeneration (Fig. 9). Residual concentration of Cd^{2+} species in the solution at the cell outlet was 1-2 mg dm^{-3}. Thus, the removal degree reached 96-98 %. Hardness ions are removed simultaneously, however, the relation of their summary molar concentration to the Cd^{2+} content was 7.4. In the case of initial solution, this ratio is 3.4.

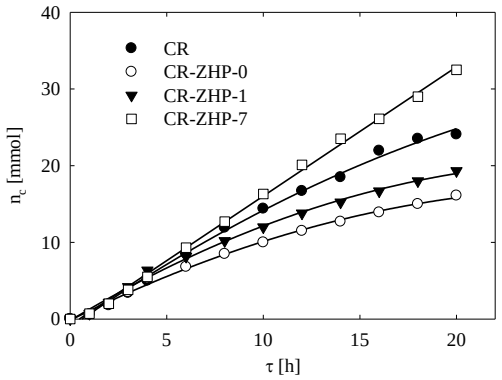

Fig. 8 Cd^{2+} amount in the catholyte as a function of time.

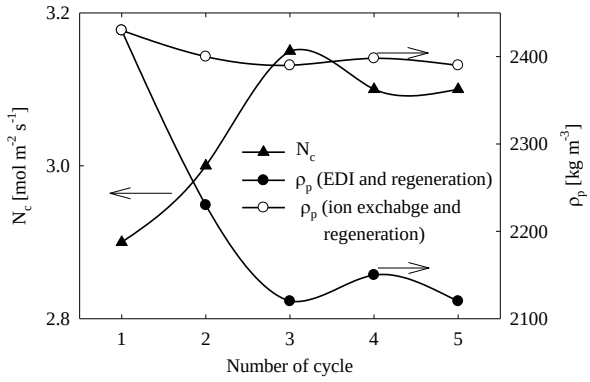

Fig. 9 Cd^{2+} flux for different cycles of EDI processes, which involve *CR-ZHP-7*, The figure also illustrates particle density of this sample from cycle to cycle of EDI-chemical regeneration and ion exchange- chemical regeneration.

The particle density decreases from the first to third cycle of EDI-regeneration. This shows a diminishing of ZHP amount inside the ion-exchanger. Further a change of particle density remains within experimental error indicating constancy of the ion-exchanger composition. No considerable change of particle density was found for the composite after each cycle of ion exchange followed by regeneration. Thus, a decrease of the modifier content is affected by electric field.

3.6 Porous Structure of Ion-Exchanger after ED Process

Fig. 10 illustrates differential pore size distributions for the *CR-ZHP-7-ED* ion exchanger. In a comparison with *CR-ZHP*-7, the maximum related to channels is shifted towards higher r values (from log r =0.04 (nm) to 0.15 (nm)) and becomes more irregular: the peak broadens up to log r =0.5 (nm). Simultaneously, sizes of clusters and voids between gel fields decreases (from log r =0, 77 (nm) to 0.44 (nm)) and from log r =1.2 to 1 (nm) respectively). The peaks, which are related to structure defects, become more expressed. In general, the pore size distribution looks similarly to that for the *CR-ZHP-1*, except the region of channels.

Cite this Article as: Y.S. Dzyazko, Y.M. Volfkovich, L.M. Ponomaryova, V.E. Sosenkin, V.V. Trachevskii, V.N. Belyakov, Composite ion-exchangers based on flexible resin containing zirconium hydrophosphate for electromembrane separation, J. Nanosci. Tech. 2(1) (2016) 43–49.

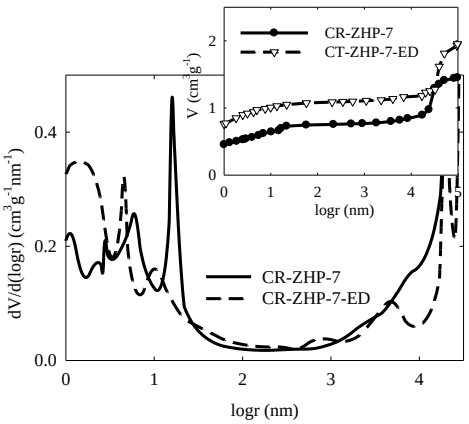

Fig. 10 Integral (insertion) and differential pore size distributions for the composite before and after 5 cycles of EDI-chemical regeneration.

Slightly higher content of free water for *CR-ZHP-7-ED* (lower water activity) as well as much lower P/P_s ratio (Fig. 6) indicates lower swelling pressure for this sample in a comparison with *CR-ZHP-7*. Higher amount of water molecules in hydrate shells of counter-ions (Table 1) is due to shrinkage of small pores. Slightly lower P:Zr molar ratio, which has been found for *CR-ZHP-7-ED*. Probably the aggregates in structure defects contain higher amount of phosphorus in a comparison with non-aggregated nanoparticles inside transport pores and voids between gel fields. Thus, destruction of the aggregates following by partial removal of the produced fragments from the ion-exchanger causes a decrease of phosphorus content. Indeed, TEM image of the *CR-ZHP-7-ED* sample shows smaller amounts of large aggregates (compare Fig. 11a and Fig. 1d). At the same time, the image of higher resolution is practically similar to that for the *CR-ZHP-7* resin (compare Fig. 11b and 1b).

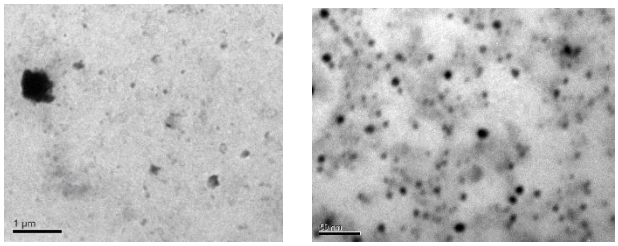

Fig. 11 TEM image of the *CR-ZHP-7-ED* sample

Thus, fragmentation of ZHP aggregates occurs during EDI processes, they partially leave the polymer phase, however, a part of them appears in widening of the smallest pores of the polymer constituent. As a result, no considerable change of electrical conductivity of the samples has been found (Fig. 7, compare *CR-ZHP-7* and *CR-ZHP-7-ED*) despite a decrease of ZHP content. The nanoparticles can move through the polymer due to electrophoresis. Moreover, the particle movement can be affected by a convective flow of the solution inside pores.

4. Conclusion

Impregnation of ion exchange resin with a $ZrOCl_2$ solution under elevated temperature allows us to obtain high amount of ZHP due to precipitation from additionally sorbed electrolyte. At the same time, a decreasing in temperature, at which precipitation occurs, promotes formation of non-aggregated nanoparticles in transport pores of the ion exchange polymer.

Insertion of the inorganic constituent into the flexible resin leads to transformation of porous structure of the polymer, this is probably due to different swelling pressure in transport and non-transport pores. From a formal point of view, modification could be considered as an increasing of the content of cross-linking agent, since the composites demonstrate more considerable swelling pressure and ion exchange capacity per volume unit in a comparison with the pristine resin. In opposite to cross-linking agent like DVB, ZHP enhances electrical conductivity of the resin. This is evidently due to participation of counter-ions of hydrophosphate groups in ion transport. Only nanoparticles in clusters contribute to the conductivity, the aggregates, which are located outside transport pores, behave as inert filler.

The composite with a maximal ZHP content provides a constancy of ion flux towards concentration compartment and high removal degree of Cd^{2+} ions during EDI process. Ca^{2+} and Mg^{2+} ions are removed simultaneously, however, they dominate in the effluent. For deeper deionization, particularly for the most complete removal of Cd^{2+} ions, reverse osmosis is recommended.

Partial release of ZHP from the ion-exchanger and redistribution of the particles inside the polymer occur during the first 40 h of the EDI process, However, no change of the composite conductivity have been found. This indicates destruction of aggregates and stability of nanoparticles in transport pores. Electrochemical method can be recommended for removal of aggregates from ion exchange material, such as organic-inorganic membranes.

Acknowledgements

The work was supported by projects within the framework of programs supported by the National Academy of Science of Ukraine "Fundamental problems of creation of new materials for chemical industry" (grant N 49/12).

References

[1] H. Strathmann, Ion-exchange membrane separation processes, Membrane Science and Technology Series, Elsevier, Amsterdam, 2004.
[2] L. Alvarado, A. Chen, Electrodeionization: principles, strategies and applications, Electrochim. Acta 132 (2014) 583–597.
[3] Ö. Arar, Ü. Yüksel, N. Kabay, M. Yüksel, Various applications of electrodeionization (EDI) method for water treatment – A short review, Desalination 342 (2014) 16–22.
[4] Ö. Arar,. Ü Yüksel, N. Kabay, M. Yüksel, Demineralization of geothermal water reverse osmosis (RO) permeate by electrodeionization (EDI) with layered bed configuration, Desalination 317 (2013) 48-54.
[5] J. Wood, J. Gifford, J. Arba, M. Shaw, Production of ultrapure water by continuous electrodeionization, Desalination 250 (2010) 973–976.
[6] P.B. Spoor, L. Grabovska, L. Koene, L.J.J. Janssen, W.R. ter Veen, Pilot scale deionisation of a galvanic nickel solution using a hybrid ion-exchange/ electrodialysis system, Chem. Eng. J. 89 (2002) 193-202.
[7] Y.S. Dzyazko, V.N. Belyakov, Purification of a diluted nickel solution containing nickel by a process combining ion exchange and electrodialysis, Desalination 162 (2004) 179-189.
[8] L.M. Rozhdestvenska, Y.S. Dzyazko, V.N. Belyakov, Electrodeionization of a Ni^{2+}-containing solution using highly hydrated zirconium hydrophosphate, Desalination 198 (2006) 247-255.
[9] H.X. Lu, J.Y. Wang, S.F. Bu, M.Q. Zhang, J.B. Zhang, Removal of nickel ions from dilute heavy metal solutions by electrodeionization process, Adv. Mater. Res. 183-185 (2011) 580-584.
[10] Y.S. Dzyazko, L.N. Ponomaryova, L.M. Rozhdestvenskaya, S.L. Vasilyuk, V.N. Belyakov, Electrodeionization of low-concentrated multicomponent Ni^{2+}-containing solutions using organic-inorganic ion-exchangers, Desalination 342 (2014) 43–51.
[11] G. Shang, G. Zhang, C. Gao, Treatment of simulated dilute Ni^{2+}-containing wastewater by electrodeionisation with a bipolar membrane: Feasibility and current density distribution, Desalination 353 (2014) 1–7.
[12] H. Lu, Y. Wang, J. Wang, Recovery of Ni^{2+} and pure water from electroplating rinse wastewater by an integrated two-stage electrodeionization process, J. Cleaner Prod. 92 (2015) 257-266.
[13] Y.S. Dzyazko, S.L. Vasilyuk, L.M. Rozhdestvenskaya, V.N. Belyakov, N.V. Stefanyak, N. Kabay, et al., Electrodeionization of Cr(VI) containing solution. Part II. Chromium transport through inorganic ion-exchanger and composite ceramic membrane, Chem. Eng. Commun. 196 (2009) 22-38.
[14] M.E.H. Bergmann, T. Iourtchouk, A. Rittel, H. Zuleeg, Feasibility studies of discontinuous electro-regeneration processes in environmentally-friendly plating for chromate separation from a binary system, Electrochim. Acta 54 (2009) 2417-2424.
[15] L. Alvarado, A. Ramírez, I. Rodríguez-Torres, Cr(VI) removal by continuous electrodeionization: Study of its basic technologies, Desalination 249 (2009) 423-428.
[16] L. Alvaradoa, I. Rodríguez-Torres, A. Chen, Integration of ion exchange and electrodeionization as a new approach for the continuous treatment of hexavalent chromium wastewater, Separ. Purif. Technol. 105 (2013) 55-62.,
[17] X. Feng, J.S. Gao, Z.C. Wu, Removal of copper ions from electroplating rinse water using electrodeionization, Jour. Zhejiang Univ. Sci. A 9 (2008) 1283-1287.
[18] Ö. Arar, Ü Yüksel, N. Kabay, M. Yüksel, Removal of Cu^{2+} ions by a micro-flow electrodeionization (EDI) system, Desalination 277 (2011) 296-300.
[19] A. Mahmoud, A.F.A. Hoadley, An evaluation of a hybrid ion exchange electrodialysis process in the recovery of heavy metals from simulated dilute industrial wastewater, Water Res. 46 (2012) 3364-3376.
[20] K.H. Yeon, S.H. Moon, A study on removal of cobalt from a primary coolant by continuous electrodeionization with various conducting spacers, Separ. Sci. Technol. 38 (2003) 2347-2371.
[21] C. Mahendra, S. Bera, C. Aanad Babu, K.K. Rajan, Separation of cesium by electro dialysis ion exchange using AMP-PAN, Separ. Sci. Technol. 48 (2013) 2473-2478.
[22] S. Gahlot, S. Sharma, V. Kulshrestha, Electrodeionization: An efficient way for removal of fluoride from tap water using an aluminum form of phosphomethylated resin, Ind. Eng. Chem. Res. 54 (2015) 4664–4671.
[23] H.J. Lee, M.K. Hong, S.H. Moon, A feasibility study on water softening by electrodeionization with the periodic polarity change, Desalination 284 (2012) 221-227.

[24] Q. Zhang, B. Pan, S. Zhang, J. Wang, W. Zhang, L. Lv, New insights into nanocomposite adsorbents for water treatment: A case study of polystyrene-supported zirconium phosphate nanoparticles for lead removal, J. Nanopart. Res. 13 (2011) 5355-5364.
[25] S. Sarkar, E. Guibal, F. Quignard, A.K. SenGupta, Polymer-supported metals and metal oxide nanoparticles: synthesis, characterization, and applications, J. Nanoparti. Res. 14 (2012) 715.
[26] Yu. Dzyazko, L.N. Ponomaryova, Y.M. Volfkovich, V.E. Sosenkin, V.N. Belyakov, Polymer ion-exchangers modified with zirconium hydrophosphate for removal of Cd^{2+} Ions from diluted solutions, Separ. Sci. Technol. 48 (2013) 2140-2149.
[27] A. Akhtar, M.D.A. Khan, S.A. Nabi, Synthesis, characterization and photolytic degradation activity of poly-o-toluidine–thorium(IV)molybdophosphate cation exchanger: Analytical application in metal ion treatment, Desalination 361 (2015) 1–12.
[28] Y.S. Dzyazko, L.N. Ponomaryova, Y.M. Volfkovich, V.V. Trachevskii, A.V. Palchik, Ion-exchange resin modified with aggregated nanoparticles of zirconium hydrophosphate. Morphology and functional properties, Micropor. Mesopor. Mater. 198 (2014) 55-62.
[29] W.Y. Hsu, T.D. Gierke, Ion transport and clustering in nafion perfluorinated membranes, J. Membr. Sci. 13 (1983) 307-326.
[30] N.P. Berezina, N.A. Kononenko, O.A. Dyomina, N.P. Gnusin, Characterization of ion-exchange membrane materials: Properties vs structure, Adv. Colloid. Interface Sci. 139 (2008) 3–28.
[31] A.B. Yaroslavtsev, V.V. Nikonenko, Ion-exchange membrane materials: Properties, modification, and practical application, Nanotech. Rus. 4 (2009) 137-159.
[32] B. Pan, Q. Zhang, W. Du, W. Zhang, B. Pan, Q. Zhang, Z. Xu, Q. Zhang, Selective heavy metals removal from waters by amorphous zirconium phosphate: Behavior and mechanism, Water Res. 41 (2007) 3103-3111.
[33] Y.S. Dzyaz'ko, V.V. Trachevskii, L.M. Rozhdestvenskaya, S.L. Vasilyuk, V.N. Belyakov, Interaction of sorbed Ni(II) ions with amorphous zirconium hydrogen phosphate, Rus. J. Phys. Chem. A 87 (2013) 840-845.
[34] F.B. Mainier, L.P.C. Monteiro, L.H. Fernandes, M.A.M. Oliveira, Restrictions on the use cadmium coating in industries, ARPN Jour. Sci. Tech. 3 (2013) 176-180.
[35] J. Rouquerol, G. Baron, R. Denoyel, H. Giesche, J. Groen, P. Klobes, et al., Liquid intrusion and alternative methods for the characterization of macroporous materials (IUPAC Technical Report), Pure Appl. Chem. 84 (2012) 107–136.
[36] Y.M. Volfkovich, V.E. Sosenkin, V.S. Bagotzky, Structural and wetting properties of fuel cell components, J. Power Sour.195 (2010) 5429-5441.
[37] N.A. Kononenko, M.A. Fomenko, Y.M. Volfkovich, Structure of perfluorinated membranes investigated by method of standard contact porosimetry, Adv. Colloid Interface Sci. 222 (2015) 425-435.
[38] Y.M. Volfkovich, V.S. Bagotsky, Experimental methods for investigation of porous materials and powders, in: Y.M. Volfkovich, A.N. Filippov, V.S. Bagotsky (Ed.), Porous materials and powders used in different fields of science and technology, Springer-Verlag, London, 2014, pp.1–8.
[39] A.D. Ward, S.W. Trimble, Environmental hydrology, Boca Raton: CTC Press LLC, USA, 2004.
[40] E. Heymann, J. O'Donnell, Physicochemical investigation of a cation exchange resin (amberlite IR100) I. Resin equilibria, J. Colloid. Sci. 4 (1949) 395–404.
[41] Y.S. Dzyazko, V.M. Linkov, V.N. Belyakov, Electrical conductivity of a flexible resin loaded with Cr (III) ions, Desalination 241 (2009) 57-67.
[42] A. Singhal, L.M. Toth, J.S. Lin, K. Affholter, Zirconium(IV) tetramer/octamer Hydrolysis equilibrium in aqueous hydrochloric acid solution, J. Am. Chem. Soc. 118 (1996) 11529-11534.
[43] A.S. Myerson, R. Ginde, in: A.S. Myerson (Ed.), Handbook of Industrial Crystallization, Butterworth-Heinemann, Woburn, 2002, pp.33-100.
[44] I. Nicotera, A. Khalfan, G. Goenaga, T. Zhang, A. Bocarsly, S. Greenbaum, NMR investigation of water and methanol mobility in nanocomposite fuel cell membranes, Ionics 14 (2008) 243–253.
[45] F. Helfferich, Ion Exchange, Dover, New York, 1995, pp.100-125.

Cite this Article as: Y.S. Dzyazko, Y.M. Volfkovich, L.M. Ponomaryova, V.E. Sosenkin, V.V. Trachevskii, V.N. Belyakov, Composite ion-exchangers based on flexible resin containing zirconium hydrophosphate for electromembrane separation, J. Nanosci. Tech. 2(1) (2016) 43–49.